Available online at www.sciencedirect.com

ScienceDirect

Ceramics International 39 (2013) 8945–8954

CERAMICS INTERNATIONAL

www.elsevier.com/locate/ceramint

Application of strontium doped calcium polyphosphate bioceramic as scaffolds for bone tissue engineering

Huixu Xie[a,1], Jianyun Wang[b,1], Chuansong Li[c], Zhipeng Gu[d], Qianming Chen[a], Longjiang Li[a,*]

[a]State Key Laboratory of Oral Diseases, West China Hospital of Stomatology, Sichuan University, Chengdu 610061, PR China
[b]Center for Human Tissue and Organs Degeneration, Shenzhen Institutes of Advanced Technology, Chinese Academy of Sciences, Shenzhen 518000, PR China
[c]Medical Scientific Academy in Sichuan People's Hospital, Chengdu 610031, PR China
[d]College of Polymer Science and Engineering, Sichuan University, Chengdu 610065, PR China

Received 29 March 2013; received in revised form 21 April 2013; accepted 24 April 2013
Available online 18 May 2013

Abstract

The critical success factors for bone tissue engineering in clinical applications are scaffolds. Ion doping is one of the most important methods to modify the properties of bioceramics for better angiogenesis abilities, biomechanical properties, and biocompatibility. This paper presents a novel ion doping method applied in calcium polyphosphate (CPP)-based bioceramic scaffolds substituted by strontium ions to form (SCPP) scaffolds for bone tissue regeneration. The microstructure and crystallization of the scaffolds were detected by scanning electron microscopy (SEM) and X-ray diffraction (XRD). Degradation tests were assessed to evaluate the mechanical and chemical stabilities of SCPP in vitro. The cell biocompatibility was measured with respect to the cytotoxicity of the extractions of scaffolds. Bone implantation was performed to evaluate the biodegradability and osteoconductivity of the scaffolds, and the bone formation examined by using X-ray radiography. The results indicated that the obtained SCPP scaffolds had a single CPP phase. The SCPP scaffolds yielded a better degradation property than the pure CPP scaffold. The MTT assay and in vivo results reveal that the SCPP scaffolds exhibited a better cell biocompatibility and tissue biocompatibility than CPP and hydroxyapatite (HA) scaffolds. The in vivo immunohistochemistry staining for VEGF also showed that SCPP had a potential to promote the formation of angiogenesis and the regeneration of bone. SCPP scaffold could serve as a potential biomaterial with stimulating angiogenesis in bone tissue engineering and bone repair.

Keywords: Strontium-doped calcium polyphosphate; Scaffolds; Angiogenesis; Bone tissue engineering

1. Introduction

Bone tissue engineering is designed to regenerate large skeletal defects. In bone tissue engineering, scaffolds play a critical role during the formation and supply of reparative cells in clinical applications. Developing controllably biodegradable materials as bone graft substitutes for filling large bone defects remains a main task in biomaterials research. In general, an ideally degradable biomaterial can controllably degrade to match the rate of new tissue regeneration. Calcium polyphosphate (CPP), a novel bioceramic as a bone substitute, has been developed since it was invented 10 years ago [1–4]. CPP has drawn attentions because of its outstanding biocompatibility [5,6], controllable degradability [7], excellent mechanical property, and compositional similarities to natural bone [8,9]. Grynpas found that the CPP scaffold supported bone in growth without an adverse reaction after it was implanted in the distal femur of rabbits [2]. This result suggested that the CPP scaffold had its potential as a bone implant material. Many in vivo experiments also indicate that the CPP scaffolds showed excellent osteoconductivity and can be used as an ideal bone substitute material [2–4].

The degradability of CPP was found to be low, which suggests that the CPP scaffolds might not match bone growth

*Corresponding author.
E-mail address: muzili63@163.com (L. Li).
[1]These authors contributed equally to this work.

0272-8842/$ - see front matter © 2013 Elsevier Ltd and Techna Group S.r.l. All rights reserved.
http://dx.doi.org/10.1016/j.ceramint.2013.04.091

rates when they are implanted in bone structures. Aimed at improving its degradability, Qiu studied the effect of ion doping in CPP on its degradability and mineralization [10]. The results indicate that the doped elements significantly affected the properties of CPP. Strontium is a bone-seeking element which presents a dual action of improving bone formation as well as inhibiting bone resorption [11]. As a result, strontium is thought to be effective in enhancing the bioactivity and biocompatibility of biomaterials. According to our previous studies, to develop new bone tissue-engineered scaffolds with angiogenic potential, we prepared strontium-doped calcium polyphosphate (SCPP).

In our previous studies, we introduced strontium into CPP to synthesize strontium-doped calcium polyphosphate (SCPP) with various crystal structures, and investigated its structures and various properties. We also researched the biocompatibility of SCPP in vitro [10], and found that SCPP containing low-dose strontium could promote osteoblasts and endothelial cells proliferation and differentiation in vitro. Chen et al. found that the degradation products of SCPP could stimulate the proliferation, migration and tube-like structure formation of endothelial cells in vitro [12,13].

However, little is known with respect to the influence of co-doped CPP structures on their microstructures, mechanical properties, and biocompatibilities. In this paper, we further studied strontium co-substituted CPP scaffolds regarding their biodegradability, biomechanical property and biocompatibility. To mimic the body conditions, we used simulated body fluid (SBF) to characterize the effects of SCPP on the degradation behavior in vitro. Proliferation of human osteoblast-like cells was used to evaluate the cell biocompatibility of SCPP in vitro. In vivo biodegradability, biocompatibility and osteogenesis property of SCPP scaffolds were investigated to use a rabbit thighbone defect model to demonstrate their potential applications as bone substitutes. The study aimed to develop new bone tissue-engineered scaffolds with angiogenic potential (e.g. SCPP scaffolds) and research the effect of SCPP scaffolds on the expression of VEGF and MMP-2.This study would provide a new kind of material with potentiality to induce bone substitute and angiogenesis for the future bone tissue-engineering.

2. Materials and methods

2.1. Preparation of porous CPP, SCPP and HA scaffolds

CPP and SCPP were synthesized by gravity sintering. The $CaCO_3$ powders was mixed with $SrCO_3$ with a molar ratio of Ca/Sr=92/8, which was the constitution of SCPP. And the one of CPP was 100% $CaCO_3$. The mixture was added slowly into the phosphoric acid (15%) and stirred before the powders dissolved completely. Then the fluid was placed at room temperature overnight. After being evaporated in vacuum, the precipitates were washed by ethanol several times until the pH of the ethanol after washing reached to about 7. These powders were calcined at 500 °C for 10 h, and heated to 1200 °C for 1 h to form molten CPP or SCPP, which would be poured directly into the ice to avoid crystallization during cooling. The amorphous CPPs or SCPPs were the ball milled and press-formed as a cylinder of 10 mm diameter and 1 mm thickness after being mixed with stearic acid which was the porogen. After sintered at 800 °C for 3 h, the porous scaffolds were obtained. The reactions were expressed as the following equations:

$$Ca(H_2PO_4)_2 \cdot \chi H_2O \longrightarrow Ca(H_2PO_4)_2 + \chi H_2O$$

$$Ca(H_2PO_4)_2 \longrightarrow CaH_2P_2O_7 + H_2O$$

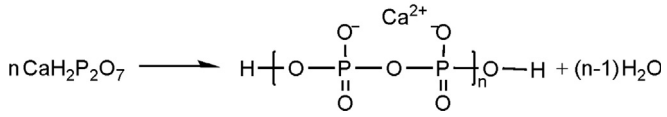

2.2. Microstructure characterization

The samples were analyzed by XRD experiments performed on the X'Pert Pro MPD X-ray diffractometer using monochromated Cu Kα radiation (Philips, Netherlands). A JEOL scanning electron microscope (JSM-5900LV) with an acceleration voltage of 20 kV was used to characterize the microstructures of two kinds of samples. The average grain sizes of the two scaffolds were determined by the lineal intercept method [14].

2.3. In vitro degradation test

In vitro degradation studies, materials were evaluated by weight-loss rate, ionic concentrations in fluid and compress test. Seven time points (0 day, 3rd day, 1st week, 2nd week, 3rd week, 4th week and 5th week) were selected as the degradation periods. The scaffolds were incubated in 15 ml SBF solution, which were prepared as Ohtsuki did [15] in sealed polyethene vials. At each time, the scaffolds were rinsed in distilled water and dried in vacuum at 50 °C before weighting. The percentage of weight loss was determined by using the following equation:

$$\text{Weightloss}(\%) = \frac{W_0 - W_t}{W_0} \times 100\%$$

where W_0 is the initial weight of the scaffold and W_t is the weight of the dried scaffold at time t. The changes of Ca^{2+} and Sr^{2+} were determined by inductively coupled plasma atomic emission spectroscopy (ICP, IRIS advantage, Thermo Elemental Co., American), respectively.

2.4. Cell culturing

Osteoblast-like ROS17/2.8 cells was selected in this study, which were made by the State Key Laboratory of Oral Diseases, Sichuan University and which was maintained at 37 °C under 5% CO_2 and 95% air in a humidified incubator. The cells were grown in DMEM medium supplemented with 10% (v/v) fetal bovine serum, 500 UI/ml of penicillin and

0.1 mg/ml of streptomycin. Fresh medium was added every 2 days.

$$Ca(H_2PO_4)_2 \cdot \chi H_2O \longrightarrow Ca(H_2PO_4)_2 + \chi H_2O$$

$$Ca(H_2PO_4)_2 \longrightarrow CaH_2P_2O_7 + H_2O$$

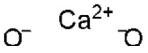

The washed samples were sterilized dry heat at 180 °C for 2 h. The sterilized materials were put into 24-well plates and immersed in 5 ml of culture medium [13]. The culture medium was removed 72 h later, and ROS17/2.8 cells at the density of 2×10^4 cm^3 were seeded directly on the surface of samples. After being cultured for 3 days, the specimens were washed four times with PBS, and fixed with 2% glutaraldehyde for 4 h at room temperature. Then samples were dehydrated in a graded series of ethanol and amyl-acetate before critical point drying [16]. SEM was used to detect attachment and morphology of cells on the material.

2.5. MTT assay

Cell proliferation was analyzed to evaluate the cytotoxicity of the SCPP, CPP and HA scaffolds by MTT (3-[4,5-dimethylthiazol-2-yl]-2, 5-diphenyltetrazolium bromide). HA scaffolds served as the control samples, which have been used as biomaterials in clinical applications. Scaffold samples with dimensions of 10-mm diameter and 1-mm length were extracted at 37 °C for 24 h in saline solution at a ratio 0.75 cm^2/mL of the scaffold samples to the volume of saline solution [16] 4×10^3 cells per well were seeded in 96-well plates after being cultured overnight. The extracts of SCPP, CPP and HA scaffolds were added into each well ($n=5$). One plate was taken out on the second, fourth and sixth days, respectively. The 20 μL/well MTT solution mixed with 5 mg/mL phosphate buffered saline (PBS) were added into the plate. The plate was incubated at 37 °C for another 4 h. After that, 150 mL dimethylsulfoxide at 300 mL/well was added to all wells and shaken for 10 min. The optical density (OD) of each well was measured by a Microplate Reader (Model550, Bio Rad Corporation) at the wavelength of 492 nm to evaluate the cell numbers which were proportional to the OD value.

2.6. In vivo implantation

The experimental animals were cared in accordance with the Principles of Laboratory Animal Care formulated by the National Society for Medical Research and the Guide for the Care and Use of Laboratory Animals published by the National Institutes of Health (NIH publication 85-23, revised 1996), and all procedures performed on animals were approved by Animal Ethics committee at Sichuan University. Twenty seven healthy New Zealand white rabbits weighting about 2.5 ± 0.4 kg each were anesthetized with pentobarbital sodium. For each rabbit, a parallel lengthwise incision was made on the back of the rabbit after a piece of skin was prepped and sterilized with iodine. For bone implantation, a defect approximately 15×5 mm^2 above the thighbone was filled with the prepared scaffold with dimensions of 15 mm × 5 mm × 4 mm (Fig. 1). Each group of rabbits was sacrificed after implantation for 4, 8 and 12 weeks. The scaffolds with surrounding tissue were excised, fixed in 10% neutral buffered formalin, decalcified and embedded in paraffin.

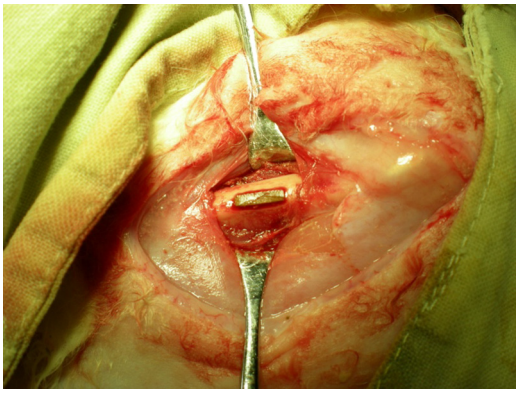

Fig. 1. A defect approximately 15×5 mm^2 above the thighbone was filled with the prepared scaffold.

To monitor the bone formation as closely as possible, some rabbits were examined using X-ray microradiography before histological study at 12 weeks. Immunohistochemical evaluation was performed using specific antibodies for VEGF and MMP-2. Immunohistochemical procedures are similar to those that are mentioned in previous investigation. Briefly, endogenous peroxidase activity was extinguished by incubation in hydrogen peroxide for 10 min. Slides were immersed in a 1 mM solution of EDTA (PH 8.0) boiled by high temperature steam for 1 min, and then cooled down. Sections were incubated with anti-VEGF or anti MMP-2 for 1 h, appropriate biotin-conjugated secondary antibody for 10 min and followed by incubation with streptavidin-peroxidase for 10 min. Finally, color was developed with fresh DAB solution for 3 min for analysis. The histological sections were observed using a light microscope (BX41, Olympus, Japan).

2.7. Image analysis

The quantification of inflammatory cells was performed by counting the number of positive cells in micrographs (× 400) taken in six areas equally distributed in the scaffold of each disk. Disks from four different animals ($n=3$) of each time point were used to calculate the mean values. All analyses and determinations were repeated at least three times by two independent investigators on blinded samples.

Quantitative determinations of newly formed bone and residual material were performed using image and statistical analysis of histological sections. In every implantation time, six pieces of histological sections were randomly chosen from K/SR-CPP, HA and CPP groups. After stained with H&E, each section was observed under a light microscope at 50 magnification and at 10 different locations selected randomly. All analyses and determinations were repeated at least three times by two independent investigators on blinded samples.

Using image analytical software Image-ProPlus (Media Cybernetics, USA), new bone volume (NBV) was expressed as the percentage of newly formed bone area in the available pore space (bone area/pore area × 100%).

2.8. Statistical analysis

Statistical analysis was performed by software SPSS19.0 (SPSS, Inc., Chicago, IL). The experimental data obtained in this paper were presented as means ± standard deviation (SD). Differences between groups were determined by one-way ANOVA, with a significance level of $p < 0.05$.

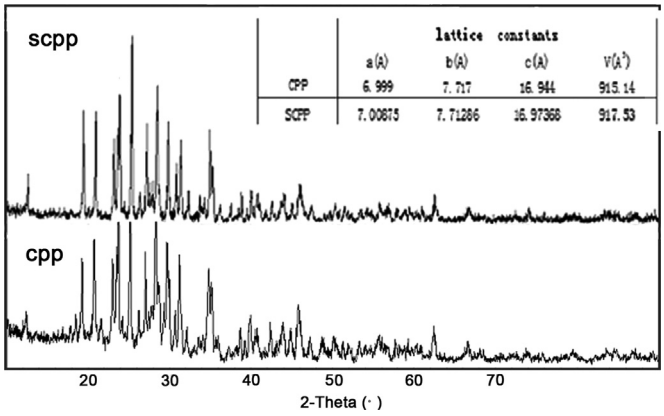

Fig. 2. XRD patterns of CPP and SCPP.

3. Results

3.1. XRD analysis

The XRD pattern of CPP and SCPP were obtained in this study. It can be seen from the XRD pattern of SCPP (Fig. 2) that the obtained sample consisted of a single CPP phase, which is confirmed from observed characteristic peaks at diffracted angles (2) 27.878°, 29.516° and 33.161°, respectively, for crystal plane (014), (022) and (122). In addition, the XRD patterns show no significant difference in crystallized phase between the CPP and SCPP, which indicated that the foreign metallic ions (Sr^{2+}) did not affect the crystallized phase of CPP structure.

3.2. Microstructure analysis

As shown in Fig. 3, the open macro-porous of the scaffolds with an interconnected porous network ranged from 100 to 400 μm. The porosity of scaffolds which was measured by liquid displacement was about 65% for all the scaffolds. Therefore, the three-dimensional and highly interconnected macro-porous network of the prepared scaffold allows not only for cell growth and spatially even distribution but also for flow transport of nutrients and metabolic waste. The major differences of three scaffolds were observed at a magnification of 5000 ×, it seems that the crystal grains of SCPP are more intimately than CPP. From the SEM micrographs, it can be seen that obvious amorphous area existed in SCPP, while the surface morphology of CPP was more density and smooth.

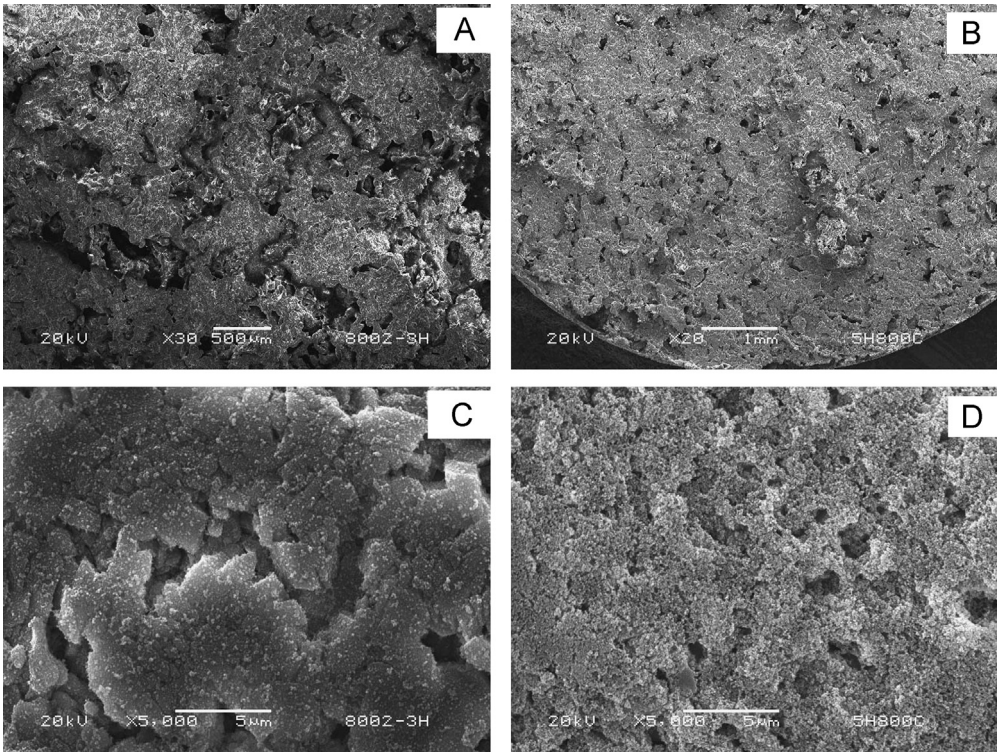

Fig. 3. SEM images of SCPP, CPP scaffolds after 5 weeks degradation in Tris A:CPP(× 30); B:SCPP(× 20); C:CPP(× 5000); D:SCPP(× 5000).

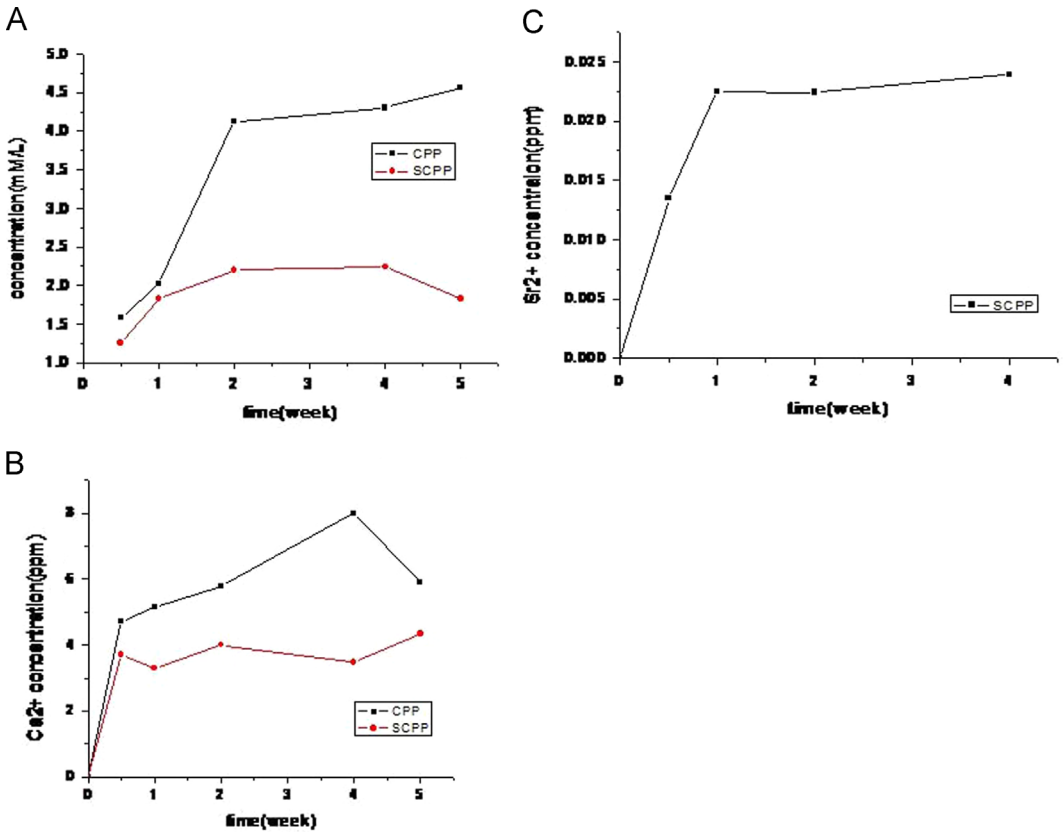

Fig. 4. (a) Ca^{2+} ion concentration (a), PO_4^{3-} (b) concentrations in SBF of CPP and SCPP and Sr^{2+} ion concentration in SBF of SCPP.

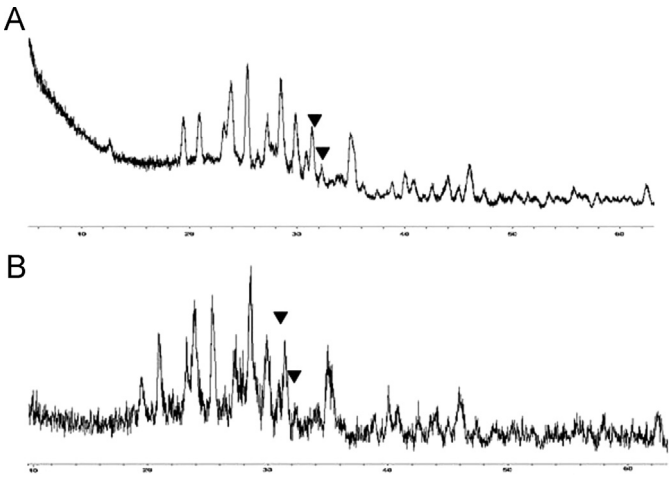

Fig. 5. XRD patterns of CPP and SCPP after 3 weeks degradation.

3.3. Degradation in SBF

The release rates of Ca^{2+} and PO_4^{3-} of CPP and SCPP scaffolds and the release rates of Sr^{2+} of SCPP are presented in Fig. 4. Both the two patterns of scaffolds exhibited an incessant increase of the Ca^{2+} and PO_4^{3-} concentrations in SBF with degradation time. But compared with CPP, the SCPP scaffold exhibited a higher degradation rate at each time points. It can be seen that the PO_4^{3-} and Ca^{2+} concentrations released into SBF of SCPP scaffold are considerably larger than that of CPP scaffold after degradation for 5 weeks. As proved by Pilliar [1], the amorphous and grain boundary regions, contained many disorder atoms or molecules, were the weakness points in CPP crystal. And the degradation media could attack these areas easily, which led to a rapid degradation in the initial period of immersion.

After 3 weeks scaffolds in SBF, CPP is confirmed from observed characteristic peaks at diffracted angles (2) 23.84°, 25.36°and 25.50°, respectively, which the highest peak locate at 25.36°. It can be seen from the XRD pattern of SCPP that the obtained samples similar with CPP phase, which the highest peak locate at 25.36° (Fig. 5). On the surface, white deposition over the surface of the scaffolds are observed in 3 weeks. A HA layer was formed on the surface, and the SCPP scaffold exhibited a higher deposition rate than the CPP scaffold (Fig. 6).

3.4. Cell attachment

Fig. 7 shows the SEM micrographs of cells spreading on samples. After 2 day of incubation, ROS17/2.8 cells were spindle-shaped and displayed elongated morphology on the specimen. After 2 days of incubation, the osteoblasts were fully spread, and mainly presented a flattened, osteoblast-like morphology. The adhered cells developed numerous cellular processes (lamellipodia and filopodia) to facilitate cell–substrate and cell–cell interactions. A large amount of lamellipodia structure was noticed in this study, which indicates the preferable, strong interactions between cells and the SCPP

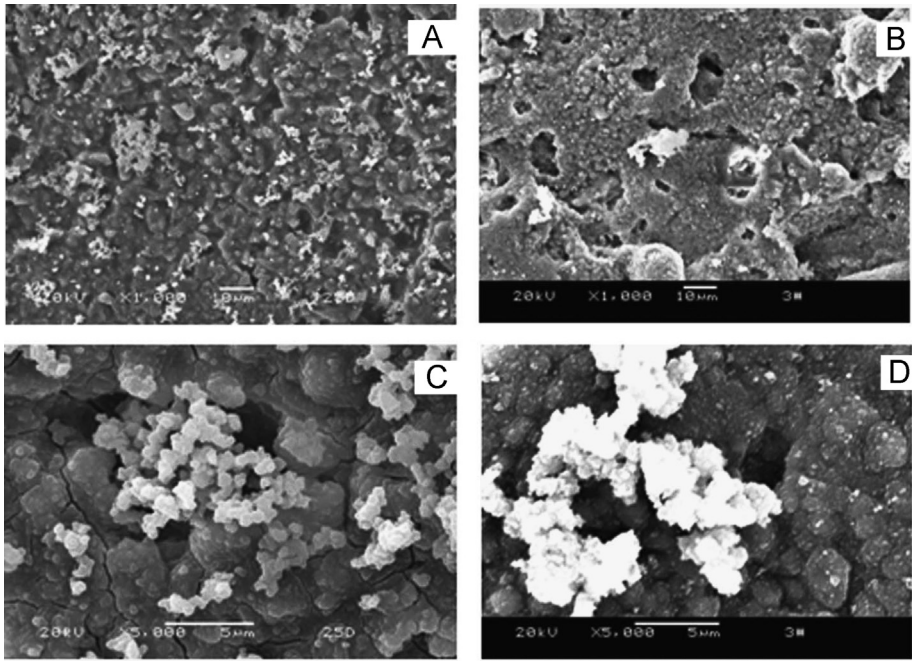

Fig. 6. SEM images of SCPP, CPP scaffolds after 3 weeks degradation in SBF A:CPP(× 1000); B:SCPP(× 1000); C:CPP(× 5000); D:SCPP(× 5000).

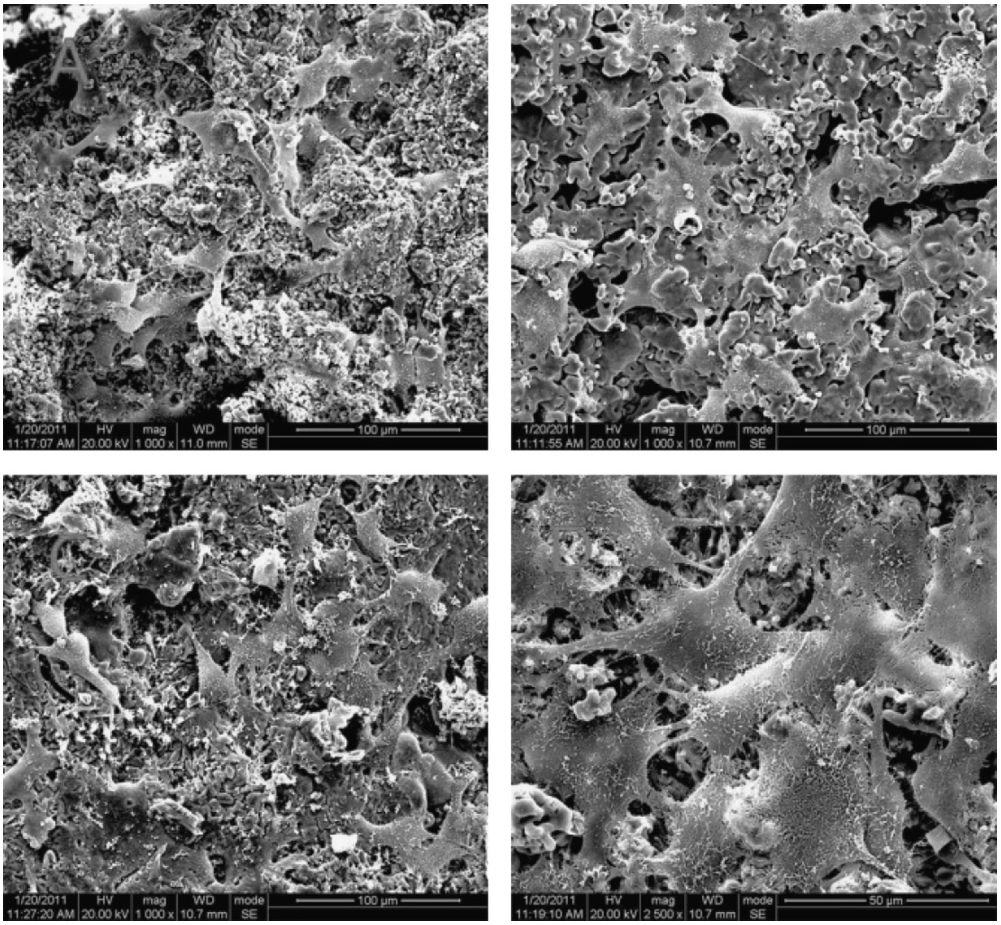

Fig. 7. The SEM micrographs of cells spreading on scaffolds A: CPP(× 500); B:HA(× 500); C:SCPP(× 500); D:SCPP(× 1000).

surface. (Fig 7C and D) and a few of adhered cells were noticed on the CPP and more less on the HA surface (Fig 7A and B). These results suggested that osteoblast-like cells can attach better on the surface of SCPP than HA and CPP, and there is no adverse cellular response to the materials.

3.5. In vitro cell proliferation

MTT assay is an important method to evaluate the cytotoxicity of the extractions of scaffolds. Fig. 8 presented the cytotoxicity result of CPP and SCPP with HA served as the control. The OD values revealed that the cell proliferation increased with the culture time on the three groups. However, it was clear that the growth rate was SCPP > CPP > HA during the entire culture period, indicating that SCPP was nontoxic. And, SCPP exhibited a better biocompatibility in vitro than CPP and HA.

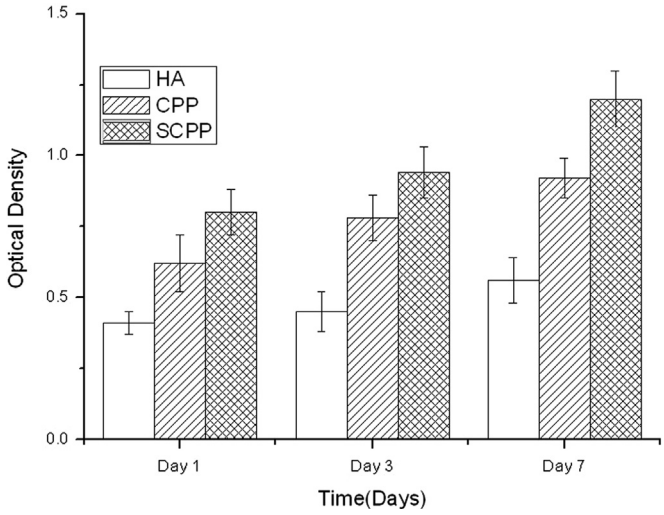

Fig. 8. MTT assay for proliferation of ROS17/2.8 cultured in the extraction of HA, CPP and SCPP for different days.

3.6. Bone implantation

In bone implantation experiment, all surgeries on the rabbits were completed successfully and the animals survived during the 12 postoperative weeks. None of the implanted sites of the rabbits showed any infection and inflammation after the operation. Fig. 9 shows optical images of MMP-2 histological staining of the HA, CPP and SCPP scaffolds after implantation. Both tissue response and degradation surrounding the scaffold could be observed.

After 4 weeks of implantation, the interface of all the scaffolds was clearly visible. New bone was observed in the margins of the implant, the scaffolds became loosen and there was no new bone formation in the center of the SCPP scaffolds. HA scaffolds did not adhere to the bone closely, which there was not the direct evidence of bone formation. New bone and bone lacuna was observed in the margins of the implant and degradation of the CPP scaffold was not observed. With the implantation prolonged, more newly formed bone tissues, The HA scaffolds-implanted produced much more variable results. In some cases, small amounts of new bone tissues formed in the scaffold. The interface between materials and tissues was still clearly visible after implantation for 8 weeks. Newly formed

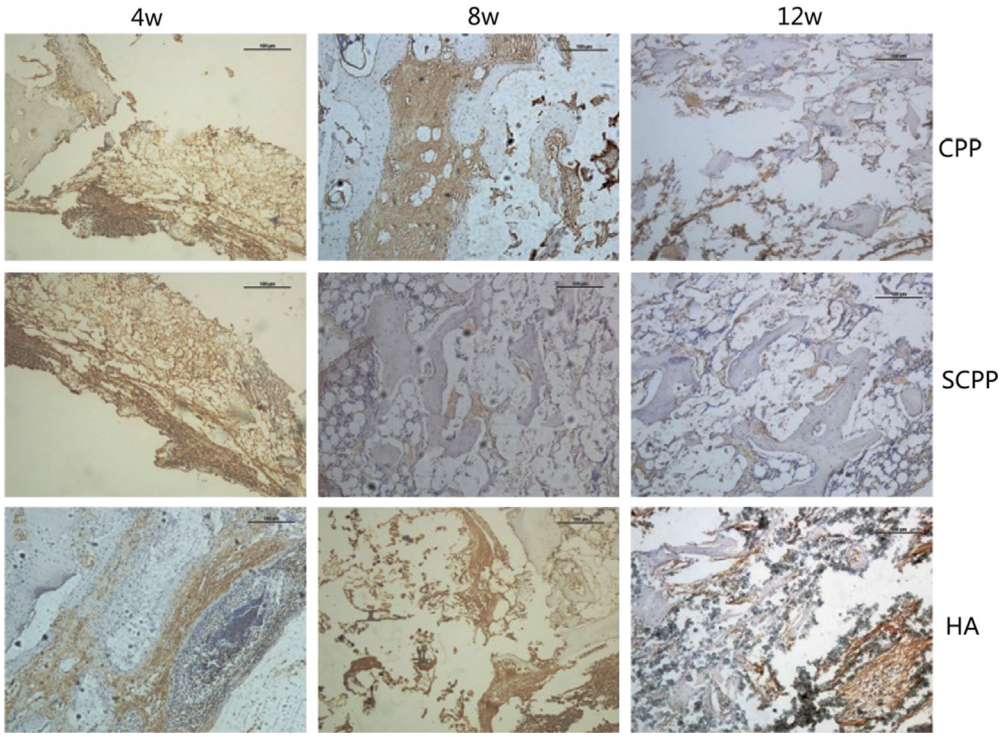

Fig. 9. Optical micrographs of MMP2-stained sections of scaffolds after implantation in rabbits (× 100).

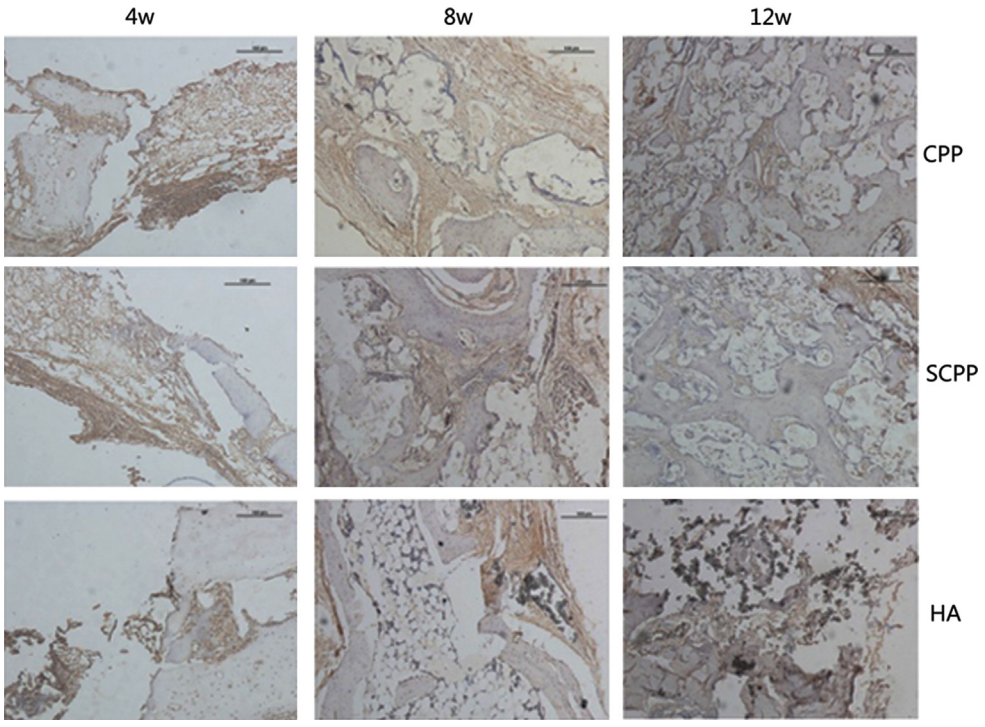

Fig. 10. Optical micrographs of VEGF-stained sections of scaffolds after implantation in rabbits (× 100).

bone tissues including bone trabecular and lacuna, were observed in the SCPP group after implantation for 8 weeks, which would accelerate the mineralization and regeneration of new bone. Small area and sporadic new bone was in the center of the SCPP scaffolds. In the CPP group, newly formed bone and lacuna increased and CPP scaffolds became loosen. Finally, after 12 weeks of implantation new bone regenerated and penetrated through the interconnective pores to the center of the scaffolds. The interface between material and host bone was hardly detectable and formed a close union in the SCPP group, and a amount new bone in the center of scaffolds with trabecular structure was consistently seen. In the case of the HA group, new bone combine with the HA scaffolds closely and the degradation of HA was only minor or virtually absent in implants during the 12 weeks analysis period. In the case of the CPP group, host bone formed a close union while the new bone regenerated and penetrated through the interconnective pores to the margin of the scaffolds.

Fig.10 shows the representative images of VEGF immunohistochemical stains of CPP, SCPP and HA scaffolds after implantation. Both bone formation and VEGF-evidence of angiogenesis in vivo in the scaffolds surrounding the scaffold could be observed.

After 4 weeks of implantation, detachments were still found at the bone–material interface in three sample groups, which there were not the evidence of angiogenesis. With the implantation prolonged, more newly formed bone tissues were seen under lower magnification. More importantly, the positive immunohistochemistry staining for VEGF was found in newly regenerated tissue in both CPP group and SCPP group after 8 weeks with more intensive positive staining in SCPP group than CPP group, and contact between bone and implant materials also became

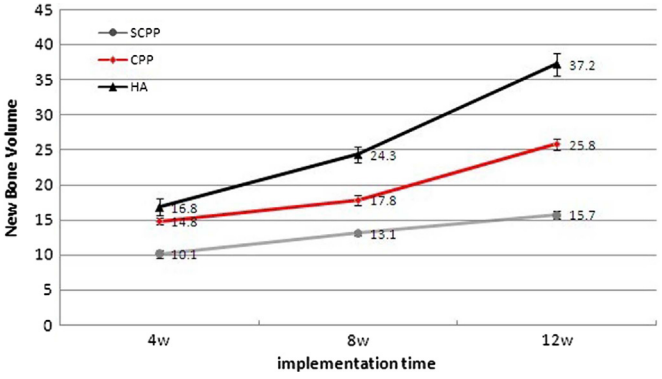

Fig. 11. Quantification of newly formed bone was performed using statistical analysis of histological sections. Error bars represent means ± SD for $n=3$.

intimate in these two groups. In contrast, the contact between bone and materials was still not close in HA group at weeks 8 and 12, and the immunohistochemistry staining for VEGF in newly regenerated tissue in HA group presented a mild positive. The intensity of positive VEGF staining increased after 12 weeks in CPP group, but decreased in SCPP group.

To quantitatively determine the amount of newly formed bone, we statistically analyzed the histological sections of different implantation periods. Fig. 11 shows new bone volume (NBV) of each implantation period. Obviously, before 8 weeks post-implantation, the amounts of newly formed bone in SCPP group increased dramatically, much more than that of CPP scaffold. After that period, however, the rate of bone formation in SCPP scaffold slowed down, while in CPP scaffold the speed of new bone formation gradually grew. In HA scaffold group the speed of new bone formation slowly grew during the 12 weeks analysis period. These results demonstrated that SCPP scaffolds presented

higher efficiency of bone formation than CPP and HA scaffolds at the long term (12 weeks analysis period).

3.7. X-ray image

X-ray microradiographic analysis confirms the results of the histological study that both the SCPP and the CPP substitutes are biocompatible and osteoconductive to the host bone. At 12 weeks post-implantation, the SCPP/bone boundary became illegible, suggesting the occurrence of mineralization and increasing density of the scaffold (Fig. 12c). The disappearance of the boundary of material and tissue indicated that the density of newly formed bone was as high as that of host bone. In CPP group, the CPP/bone boundary was legible, suggesting the rate of bone formation and scaffold degradation in CPP scaffold was slow, a lower compressive strength and a worse degradation property than the SCPP scaffold (Fig. 12B). In HA group, the HA/bone boundary was quite legible, a little scaffold degradation was observed in X-ray image (Fig. 12A).

4. Discussions

Degradability is one of important properties of bone implant materials because it is crucial for bone induction, conduction, metabolism and longevity when implanted into body. In general, materials should be controllable degradation to match the rate of new tissue regeneration. For CPP, the degradation behavior in vitro may be the result of physical abrasion and chemical dissolution. Firstly, the physical factors, such as porosity, crystallinity and grain size, could affect the abrasion, fracture and disintegration process when CPP was immersion in degradation media. Secondly, chemical factor included on composition and ionic substitutions in materials play an important role in the degradation behavior of CPP in vitro. In previous study, our group had focused on the physical and chemical degradation of CPP and found the crystal structure [17], sintering time and temperature [11], polymerization degree [7], ion doped [10] and degradation media [18] can control its degradation process (Fig. 3c).

There are many factors that can influence the cell behavior on materials, such as surface chemistry, surface roughness, surface energy and so on. Bioactive materials, and particularly bioactive glass–ceramics undergoing corrosion in aqueous solution, create a microenvironment that can influence cell response. Additional experiments must be performed for a better understanding of the relationship between SCPP and cells cultured on its surface.

It had been proved that Sr^{2+} had the ability to enhance bone cell replication and bone formation in vitro. Qiu had found that SCPP could promote the growth and adhesion of osteoblasts in vitro [10]. The doped Sr ions improved the cell biocompatibility of SCPP scaffold.

The course of the foreign body reaction (FBR) against scaffolds implants as showed in the histochemical staining on plastic embedded sections. The degradation of HA was only minor or virtually absent in implants during the 12 weeks analysis period. The degradation of CPP was slow in implants during the 12 weeks analysis period. In contrast, the degradation of SCPP had commenced at week 4, although only a few cells had infiltrated. The degradation had advanced at week 8 and was characterized with increased cellular influx surrounding the scaffolds. Within 12 weeks, the majority of SCPP been degraded. It was clear that the degradation rate was SCPP > CPP > HA during the entire period, while the rate of new bone formed was SCPP > HA > CPP during the entire period.

The bioactivity of scaffolds to induce angiogenesis in vivo was usually evaluated through assessing the ability of scaffolds to stimulate the release of angiogenic growth factors from host

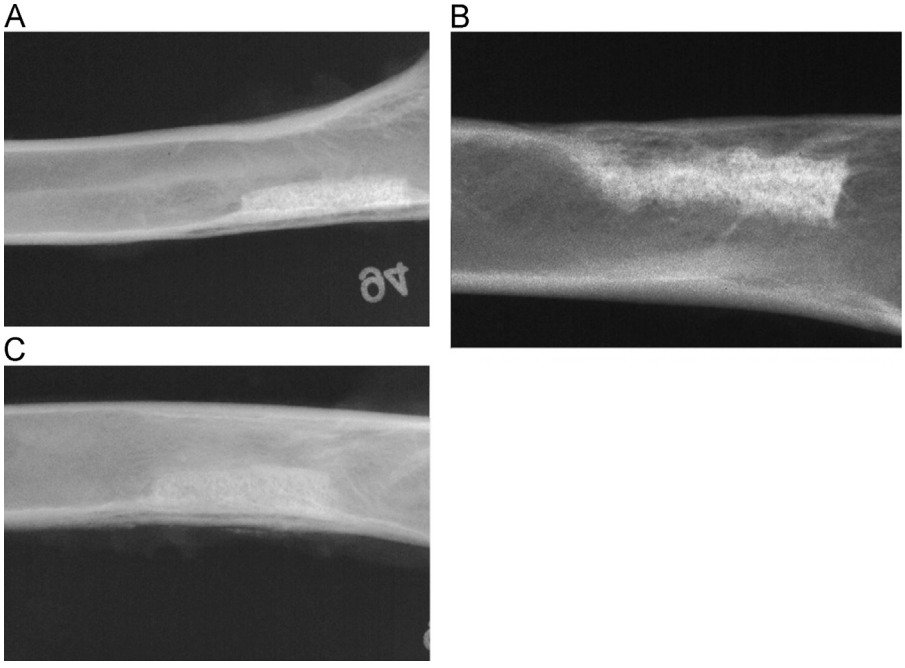

Fig. 12. X-ray microradiographic analysis after 12 weeks.

cell. Matrix metalloproteinase-2 (MMP-2) is one of the important factors resulting in tumor angiogenesis by means of degrading extracellular matrix and basement membrane, facilitating the migration of endothelium cells [19]. Vascular endothelial growth factor (VEGF), as a critical regulator in physiological angiogenesis, is one of the most potent inducers of angiogenesis and plays a significant role in skeletal growth and repair [20]. Therefore, the expression of MMP-2 and VEGF has become an important indication which measures the ability of scaffolds to induce angiogenesis in vivo. In this study, a different expression pattern of MMP-2 and VEGF was observed in three sample groups. The expression of MMP-2 and VEGF within SCPP scaffold is significantly higher and more widely and evenly distributed than CPP and HA scaffold during the early post-operation periods. MMP-2 and VEGF expression in newly regenerated bone tissues has been week in HA group. The surface chemistry, structure and porosity of biomaterials are known to affect cell-specific functions such as the expression of cytokine and growth factor [21]. In our study, the incorporation of strontium into CPP changed the surface topography and made SCPP possessed a smoother surface as well as a more compact bulk, which might up-regulate the expression of MMP-2 and VEGF. Most importantly, Sr released from SCPP scaffold might promote a higher MMP-2 and VEGF expression of host cells, which might lead to more cell infiltration, more extracellular matrix synthesis, faster angiogenesis and more excellent repair of bone defect in vivo. In addition, we also found in this study that SCPP can significantly promote the new bone formation, and the bone-materials interface in the SCPP group is better than CPP and HA group. In agreement with our previously investigation, SCPP scaffolds could be a good promise materials with ability to induce angiogenesis for the bone tissue-engineering.

5. Conclusion

To our knowledge, the SCPP scaffolds studied in this paper is a good kind of bioceramic bone repair scaffold to demonstrate the potential to complete bone repair and stimulate angiogenesis. This study might provide a fast and effective way to promote the osteogenesis and angiogenesis for bone repairing, with great clinical potentials for the large bone defect treatment.

Acknowledgments

This work was supported by the National Natural Science Foundation of China (81172578).

References

[1] R.M. Pilliar, M.J. Filiaggi, J.D. Wells, M.D. Grynpas, R.A. Kandel, Porous calcium polyphosphate scaffolds for bone substitute applications—in vitro characterization, Biomaterials 22 (2001) 963–972.

[2] M.D. Grynpas, R.M. Pilliar, R.A. Kandel, R. Renlund, M. Filiaggi, M. Dumitriu, Porous calcium polyphosphate scaffolds for bone substitute applications in vivo studies, Biomaterials 23 (2002) 2063–2070.

[3] T.Y. Sayegh, R.M. Pilliar, C.A. McCulloch, Attachment, spreading, and matrix formation by human gingival fibroblasts on porous-structured titanium alloy and calcium polyphosphate substrates, Journal of Biomedical Materials Research A 61 (2002) 482–492.

[4] S.D. Waldman, M.D. Grynpas, R.M. Pilliar, R.A. Kandel, Characterization of cartilagenous tissue formed on calcium polyphosphate substrates in vitro, Journal of Biomedical Materials Research 62 (2002) 323–330.

[5] E.K. Park, Y.E. Lee, J.Y. Choi, S.H. Oh, H.I. Shin, K.H. Kim, et al., Cellular biocompatibility and stimulatory effects of calcium metaphosphate on osteoblastic differentiation of human bone marrow-derived stromal cells, Biomaterials 25 (2004) 3403–3411.

[6] S.M. Yang, S.Y. Kim, S.J. Lee, Y. Ku, S.B. Han, C.P. Chung, Tissue response of calcium polyphosphate in Beagle dog. Part II: 12 month result, Key Engineering Materials 218 (2004) 657–660.

[7] Y.L. Ding, Y.W. Chen, Y.J. Qin, G.Q. Shi, X.X. Yu, C.X. Wan, Effect of polymerization degree of calcium polyphosphate on its microstructure and in vitro degradation performance, Journal of Materials Science: Materials in Medicine 19 (2008) 1291–1295.

[8] F. Gomez, P. Vast, P. Llewellyn, F. Rouquerol, Dehydroxylation mechanisms of polyphosphate glasses in relation to temperature and pressure, Journal of Non-Crystalline Solids 222 (1997) 415–421.

[9] A.G. Dias, M.A. Lopes, I.R. Gibson, J.D. Santos, In vitro degradation studies of calcium phosphate glass ceramics prepared by controlled crystallization, Journal of Non-Crystalline Solids 330 (2003) 81–89.

[10] K. Qiu, C. Wan, C. Zhao, X. Chen, C. Tang, Y. Chen, Fabrication and characterization of porous calcium polyphosphate scaffolds, Journal of Materials Science 41 (2006) 2429–2434.

[11] W. Zhang, Y. Shen, H. Pan, K. Lin, X. Liu, B.W. Darvell, W.W. Lu, J. Chang, L. Deng, D. Wang, W. Huang, Effects of strontium in modified biomaterials, Acta Biomaterialia 7 (2011) 800–808.

[12] Y.W. Chen, T. Feng, G.Q. Shi, Interaction of endothelial cells with biodegradable strontium-doped calcium polyphosphate for bone tissue engineering, Applied Surface Science 255 (2008) 335.

[13] Y.W. Chen, G.Q. Shi, Y.L. Ding, X.X. Yu, X.H. Zhang, C.S. Zhao, C. X. Wan, In vitro study on the influence of strontium-doped calcium polyphosphate on the angiogenesis-related behaviors of HUVECs, Journal of Materials Science: Materials in Medicine 19 (2008) 2655–2662.

[14] J. Wurst, J. Nelson, Lineal intercept technique for measuring grain size in two phase polycrystalline ceramics, Journal of the American Ceramic Society 55 (1972) 109.

[15] C. Ohtsuki, H. Kushitani, T. Kokubo, S. Kotani, T. Yamamuro, Apatite formation on the surface of ceravital-type glass-ceramic in the body, Journal of Biomedical Materials Research 25 (1991) 1363–1370.

[16] C. Fiske, Y. Subbarow, The colorimetric determination of phosphorus, Journal of Biological Chemistry 66 (1925) 37.

[17] K. Qiu, C. Wan, X. Chen, Q. Zhang, H. Su, In vitro degradation studies of calcium polyphosphate ceramics prepared by controlled degree of polymerization and crystallization, Advanced Biomaterials VI 288–289 (2005) 553–556.

[18] Q. Wang, J. Wang, X. Zhang, et al., Degradation kinetics of calcium polyphosphate bioceramic: an experimental and theoretical study, Materials Research 12 (2009) 495–501.

[19] L. Heckmann, H.J. Schlenker, J. Fiedler, R. Brenner, M. Dauner, G. Bergenthal, et al., Human mesenchymal progenitor cell responses to a novel textured poly(L-lactide) Scaffold for ligament tissue engineering, Journal of Biomedical Materials Research Part B: Applied Biomaterials 81B (2007) 82–90.

[20] J. Street, M. Bao, L. deGuzman, S. Bunting, F.V. Peale Jr., N. Ferrara, et al., Vascular endothelial growth factor stimulates bone repair by promoting angiogenesis and bone turnover, Proceedings of the National Academy of Science USA 99 (2002) 9656–9661.

[21] R.E. Unger, A. Sartoris, K. Peters, A. Motta, C. Migliaresi, M. Kunkel, et al., Tissue-like self-assembly in cocultures of endothelial cells and osteoblasts and the formation of microcapillary-like structures on three-dimensional porous biomaterials, Biomaterials 28 (2007) 3965–3976.